Dynamic Subcarrier Allocation for P2MP Connections

H. Shakespear-Miles*, M. Ruiz, and L. Velasco
Optical Communications Group (GCO), Universitat Politècnica de Catalunya (UPC), Barcelona, Spain
e-mail: hailey.shakespear@upc.edu

ABSTRACT
This paper proposes a solution for dynamically allocating subcarriers in a point-to-multipoint connection in the upstream direction. Using Digital Subcarrier Multiplexing a single carrier can be divided into several subcarriers. An ILP was proposed to dynamically allocated subcarriers in various traffic scenarios allowing for an increased number of edge nodes serviced. Significant capital and energy cost reductions were shown in comparison to traditional methods.
Keywords: digital subcarrier multiplexing, point-to-multipoint connections.

2023 23rd International Conference on Transparent Optical Networks (ICTON) | 979-8-3503-0303-2/23/$31.00 ©2023 IEEE | DOI: 10.1109/ICTON59386.2023.10207298

1. INTRODUCTION

Digital Subcarrier Multiplexing (DSCM) systems bring large efficiency and cost reduction for access/metro applications, as they use multiple subcarriers (SC), e.g., 4, 8 or more, instead of a single one [3]. In typical point-to-point (P2P) systems, the DSCM is realized at the transmitter (Tx) side and each SC is individually detected and post-processed at the coherent receivers (Rx). However, point-to-multipoint (P2MP) connectivity is also possible, which would be beneficial to support of advanced 5G and 6G infrastructure [4]. In the architecture proposed by the authors in [4], a number of edge nodes communicate with a single hub; in the upstream direction, the SCs generated by the edge nodes were all aggregated at the hub, whereas in the downstream direction, the SCs generated by the hub were received by the edge nodes. In such architecture, each edge node had assigned a subset of SCs, thus creating P2P pipes inside a P2MP optical connection.

A P2MP approach can result into large capital cost reduction coming from the reduction in the number of devices in the hub node. Cost reduction can be made even larger in dynamic traffic scenarios, where not all the SCs need to be active, i.e., during some time intervals when the traffic decreases. Such dynamic spectrum allocation can result in an increment on the number of edge nodes that can be supported in the P2MP connection. In addition, the authors in [5] showed that important energy savings can be obtained by activating only the SCs needed to support the current traffic.

This paper summarizes the approaches found in [1] and [2], where the focus was on proving dynamic spectrum allocation to the edge nodes for more efficient P2MP connectivity using centralized and distributed methods respectively. Owing to the fact that several Txs can request allocating new SCs for the incoming traffic, in this paper we solve this problem assuming a centralized network controller. Both a simple and efficient Integer Linear Programming (ILP) model and a deterministic algorithm are proposed to find the optimal spectrum allocation for the edge nodes. In this regard, we focus on the upstream direction, that we call multipoint-to-point (MP2P), where the edge nodes (Tx) demand a variable number of SCs as a function of the local traffic being conveyed to the hub node (Rx). Note that this problem is more complex than that for the downstream direction, where only the hub node manages the spectrum allocation.

2. DYNAMIC SC ALLOCATION FOR P2MP CONNECTIVITY

Figure 1a illustrates a MP2P optical connection based on DSCM, where n Txs at the edge nodes communicate with a single Rx at the hub node. Every Tx has a portion of the spectrum, i.e. wavelengths, assigned (dotted lines), where its SCs are allocated. The SCs of every Tx are aggregated using, e.g., an optical coupler. It is worth noting that Rx needs to support the aggregated number of SCs. A possible example would be 4 Tx supporting 4 SCs each, and one Rx supporting 16 SCs in total. Although it would be possible that the Tx could allocate every SC in a different part of the optical spectrum, we assume that this is not possible, to reduce the cost of the Tx, and all the SCs need to be allocated in a small portion of the spectrum, named channel, with minimum width to support the required SCs.

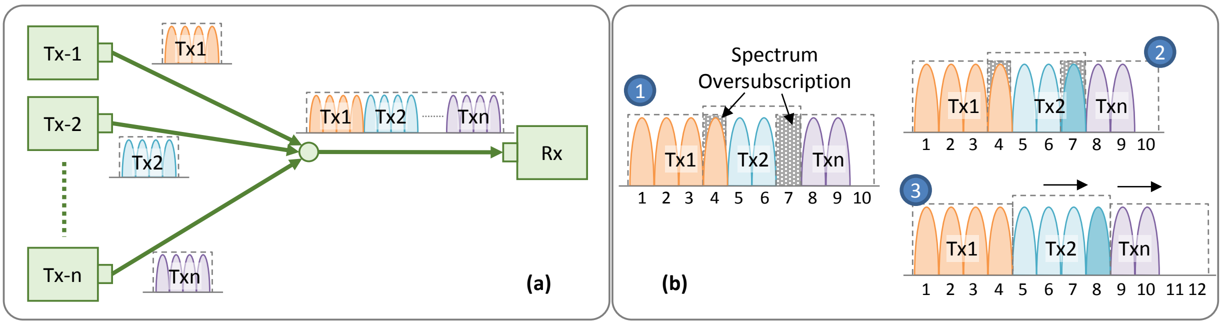

Figure 1. MP2P connectivity based on DSCM (a) and dynamic SC allocation and reconfiguration.

Figure 1b summarizes our approach, where the channel assigned to every Tx might overlap with that of other Tx; we name this spectrum oversubscription. The objective is to increase the number of Txs participating in the MP2P connection. In the first case in Fig. 1b (labeled 1), spectrum oversubscription is observed between the channel assigned to Tx1 and Tx2 (wavelength 4), as well between Tx2 and Txn (wavelength 7). Note that Tx1 has a SC active in wavelength 4, whereas wavelength 7 is not in use. Let us imagine that Tx2 needs to allocate a new SC to cope with some increment of traffic. Such SC must be allocated inside the assigned channel, which in this case is possible as wavelength 7 was available (2). At this time, Tx2 cannot allocate new SCs since all the wavelengths in the assigned channel are being used. Therefore, a reconfiguration in the neighboring assigned channel (that for Tx1 or Txn) can be tried. In (3), the channel assigned to Txn has been reconfigured, as well as the allocated SCs (SC in wavelength 8 has been deactivated and SC in wavelength 10 activated). In consequence, wavelength 8 has been released and a SC Tx2 can allocate the needed SC.

3. MODELS

This section proposes a centralized ILP and decentralized protocol to dynamically solve SC allocation and reconfiguration. The problem statement is:

Given:

- the total spectrum available for the MP2P connection, represented by ordered set $W = \{w_1, w_2, \ldots, w_{|W|}\}$, where $|W|$ is the maximum number of wavelengths supported by the Rx.
- the set of candidate channels described by set $C = \{c_0, c_1, c_2, \ldots c_{|C|-1}\}$, where c_0 is the empty set and every c_i (i:1..|C|-1) is a subset of contiguous wavelengths of size 1..m, being m the maximum number of wavelengths supported by each Tx. We assume all Tx with the same characteristics.
- a set of Txs $T=\{t_i, t_2, .., t_n\}$, where every Tx t has an associated capacity requirement k_t.

Output: the configuration of every wavelength and its assignment to every Tx, and the channel assigned to every Tx. Objectives: 1) minimize the amount of lost traffic, 2) to minimize the number of used SC, thus minimizing energy cost, 3) minimize the number of SCs that are reconfigured

The parameters and decision variables of the problem are:

α_i	Weights of the multi-objective function
k_c	Capacity of channel c
δ_{tc}	Equal to 1 if channel c is a candidate for transponder t, 0 otherwise.
v_{tc}	Total number of active wavelengths w in channel c for transponder t.
r_{tc}	Whole number describing the number of wavelengths w, that were modified with respect to c_t.
c_t	Current channel selected for transponder t.
u_{tc}	Whole number describing the difference between k_t and k_c.
δ_{cw}	Equal to 1 if wavelength w is in use for candidate channel c, 0 otherwise.
s_{tw}	Equal to 1 if Tx t current occupies wavelength w; 0 otherwise.
x_{tc}	Binary decision variable, equal to 1 if channel c is assigned to Tx t; 0 otherwise.

In order to ensure fast computation time, a pre-calculation following a similar approach than in [6] was performed, where the set of channels C is calculated as $\delta_{tc} = 1, \forall t \in T, c \in C \mid overlap(s_{tw}, c_t) \mid\mid c == c_0$ and δ_{cw} can be easily calculated for the channels. Additionally, we compute $u_{tc} = \max(k_t - k_c, 0), \forall t \in T, c \in C \mid \delta_{tc} = 1$ to calculate the traffic that could be lost, $v_{tc} = |c|, \forall t \in T, c \in C$ to track the number of wavelengths in use, and $r_{tc} = |\, index(c_t) - index(c)|, \forall t \in T, c \in C$ to measure the number of SC reconfigurations made for a potential new channel.

The mathematical programming formulation for the problem is as follows, where the objective function (eq. (1)) minimizes the three defined objectives, which are weighted by the α_i parameters, where $\alpha_1 > \alpha_2 > \alpha_3$ to maintain the priority of the objectives. Constraint (2) ensures that only one Tx can be assigned to one eligible channel, and constraint (3) ensures that every wavelength can be occupied with, at most, one and only one SC from one single Tx.

$$\min \sum_{t \in T} \sum_{c \in C} [\alpha_1 \cdot u_{tc} + \alpha_2 \cdot v_{tc} + \alpha_3 \cdot r_{tc}] \cdot x_{tc} \quad (1)$$

subject to:

$$\sum_{c \in C} \delta_{tc} \cdot x_{tc} = 1 \quad \forall t \in T \quad (2)$$

$$\sum_{t \in T} \sum_{c \in C} \delta_{tc} \cdot \delta_{cw} \cdot x_{tc} \leq 1 \quad \forall w \in W \quad (3)$$

We also define agent architecture for a decentralized MAS system using deterministic policies to organize the subcarriers in the spectrum. The agent architecture is shown in Fig. 2 where the capacity manager is charge of managing the capacity available between the local Tx and the Rx to follow traffic dynamicity. Tx and Rx agents also interact with the *transponder agent* responsible for SC operation, like activation and deactivation to meet capacity requirements, but it does not make any decisions on the use of the spectrum. The spectrum management role is now played by the MAS Rx agent contained in the Rx agent. The Tx agent also contains a MAS agent used for communication with the other MAS agents in the system. The behavior of each Tx agent is described in Algorithm 1. Pending actions are processed back after SCs are actually activated or deactivated (lines 1-4). In addition, the Rx agent maintains an internal table with the status of every SC, which is checked and updated when a request to release a SC or to get a free SC is received from a neighboring Tx agent.

When a SC release request is received (lines 5-7), the Rx agent finds which is the best SC to release as a function of the allocation of neighboring Txs. The SC selected is returned to be sent to the requesting Tx agent. The allocation of a new SC entails a more complexity (lines 8-14). If a neighboring SC to the Tx current allocation is free, then it is selected (lines 9-10). Otherwise, a possible spectrum shifting (entailing the activation and deactivation of two SCs) of a neighboring Tx is evaluated (lines 11-14). If a spectrum shifting is possible, it is requested to that Tx agent and the current SC allocation request is added to the pending list.

Keeping the spectrum allocated to the different Txs as separated as possible would allow not only quicker SC allocation as shifting might be avoided, but also reducing the possibility of SC request blocking coming from the impossibility to do shifting involving one single Tx. Then, the Rx agent pays special attention to the spectrum allocation every time any SC operation is performed (line 4).

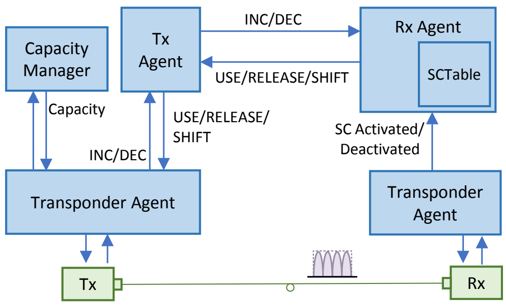

Figure 2 Agent structure and connections for decentralized operation.

INPUT: cmd, TxId	**OUTPUT:** cmd, TxId, SCId
1:	**if** cmd in {SCActivated, SCDeactivated} **then**
2:	<cmd, TxId> ← pendingReq.remove()
3:	**if** cmd is none **then**
4:	**return** reoptimizeSpectrum()
5:	**if** cmd == DEC **then**
6:	SCId ←find_best(SCTable, TxId, RELEASE)
7:	**return** {RELEASE, TxId, SCId}
8:	**if** cmd == INC **then**
9:	SCId ← find_best(SCTable, TxId, USE)
10:	**if** SCId <> -1 **then return** {USE, TxId, SCId}
11:	shift=<TxId, dir> ← find_neighborShift (SCTable, TxId, SHIFT)
12:	**if** not shift **then return** {USE, TxId, -1}
13:	pendingReq.add(<cmd, TxId>)
14:	**return** {SHIFT, shift.TxId, shift.SCId}

Algorithm 1

4. RESULTS

A simulation scenario was set up following a similar architecture that that outlined in Fig. 1, with up to 8 Txs and 1 Rx; Txs can support up to 4 SCs and the Rx up to 16 SCs. For simulation purposes we assumed that every SC is configured with 16QAM, 11 Gbaud, and 60 Gb/s capacity. The simulator was developed in Python using the PuLP package for solving the ILP problem. To simplify the discussion, we consider two extreme scenarios with Txs with traffic following similar daily patterns (see Fig. 3); in Fig. 3a the traffics are almost in-phase, whereas in Fig. 3b they are in opposite phase. To study the effects, we define traffic multiplexing ratio as a way to quantify the phase synchronization of the traffics generated by the Tx (0 ≡ in-phase and 1 ≡ opposite-phase). Note that the traffic volume in the peak entails that Txs will require allocating 4 SCs.

In Fig. 4 the dynamic SC allocation was compared against a static SC allocation in which a maximum of 4 SCs would be used by each Tx, independently of the traffic seen. Additionally, contiguity was relaxed in the ILP model for comparison purposes, representing a bound for the reallocation method. The proportion of lost traffic (traffic rejected over incoming traffic) for the almost in-phase traffic scenario is presented in Fig. 4a. As for the static method (not shown in the figure), the dynamic and bound ones are able to support 4 Txs without loss. Traffic loss appear when the number of Txs increases, since all the Tx require allocating 4 SCs simultaneously. Interestingly, the dynamic and bound methods are able to support 5 Txs without traffic loss under the opposite phase traffic scenario in Fig. 4b. The inset in the figure summarizes the gain w.r.t. the static method in terms of number of Txs and supported traffic. Figures 4c-4d show the average number of SC reconfigurations per Tx to avoid conflicts from spectrum oversubscription. Under the opposite phase traffic scenario, about 10 reconfigurations were necessary to support 5 Txs without traffic loss. Hence, a relatively small number of reconfigurations translates to a large amount of gain. To further explore the influence of the traffic multiplexing ratio together with the peak traffic volume, other traffic scenarios were examined.

We can then test the decentralized algorithm using the same traffic multiplexed ratios. Figure 5a shows the proportion of lost traffic in the in-synch traffic scenario, while (b) shows the out of synch traffic. In (a) the difference between the centralized and Rx modes is less significant, with the shifting and complete modes approaching the bound. The difference between modes is much clearer for the out of synch scenario where the complete and shifting methods are able to get much closer to the bound. Figures 5c and 5d show the number of reconfigurations by the agents for both traffic types. In the out-of-synch scenario the number of reconfigurations is overall higher for all modes, as the Rx has more options for satisfying Tx requests. It is interesting to note that the shifting mode produces a similar number of reconfigurations as the basic mode, while producing less loss while in operation.

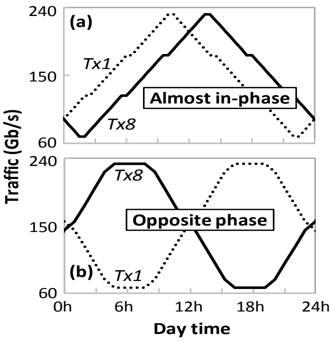

Figure 3. Traffic scenarios.

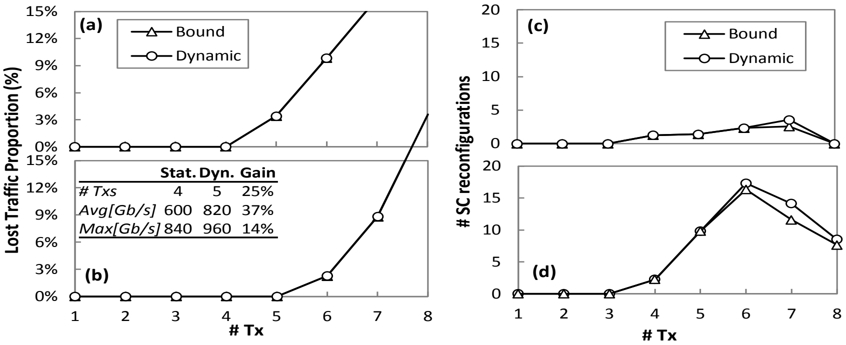

Figure 4. Dynamic vs static performance analysis.

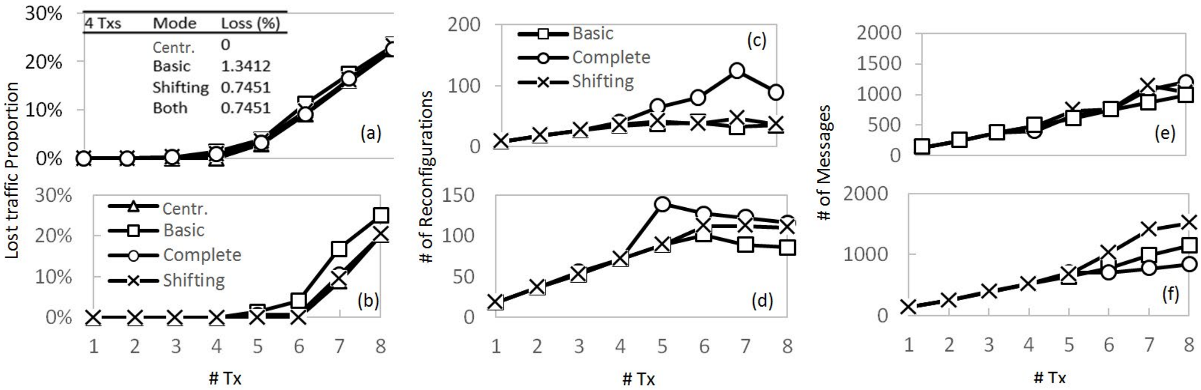

Figure 5. Decentralized MAS performance for traffic scenarios.

Associated to reconfigurations is the communication necessary for them to be performed. In Fig. 5e and 5f we can see the number of messages sent between the Tx and Rx agents. In the out-of-synch traffic scenario it is clear that for high number of SCs, more messages are necessary for the shifting method. This is not true for the complete method. If limited communications are to be considered the complete method could prove superior as it produces a very similar loss proportion with less messages.

5. CONCLUSION

We observed that imposing contiguity constraints to the Tx does not affect the benefits from the dynamic SC allocation. Hence, imposing such constraint can potentially bring cost reduction from the simplification of the Tx design. Additionally, the decentralized MAS has shown to be an adequate method for avoiding oversubscriptions in the optical spectrum of a P2MP connection. It has shown to perform comparably to centralized mitigation, while providing the added advantage of introducing scalability to near real-time operation.

ACKNOWLEDGEMENTS

This project has received funding from the Smart Networks and Services Joint Undertaking under the European Union's Horizon Europe research and innovation programme under Grant Agreement No. 101096120 (SEASON), from the MICINN IBON (PID2020-114135RB-I00) project and from the ICREA Institution.

REFERENCES

[1] H. Shakespear-Miles, M. Ruiz, A. Napoli, and L. Velasco, “Dynamic subcarrier allocation for multipoint-to-point optical connectivity,” in *Proc. 2022 27th OptoElectronics and Communications Conference (OECC) and 2022 International Conference on Photonics in Switching and Computing (PSC)*, Toyama, Japan, 2022, pp. 1-4: doi: 10.23919/OECC/PSC53152.2022.9850069.

[2] H. Shakespear-Miles, M. Ruiz, A. Napoli, and L. Velasco, “Multi-agent-based dynamic optical subcarrier allocation for near real-time P2MP operation,” in *Proc. European Conference on Optical Communication (ECOC) 2022*, paper Tu5.44.

[3] T. Rahman *et al*., “Digital subcarrier multiplexed hybrid QAM for data-rate flexibility and ROADM filtering tolerance,” in *Proc. OFC*, 2016.

[4] D. Welch *et al*., “Point-to-multipoint optical networks using coherent digital subcarriers,” *IEEE/OPTICA Journal of Lightwave Technology*, vol. 39, pp. 5232 - 5247, 2021.

[5] L. Velasco *et al*., “Autonomous and energy efficient lightpath operation based on digital subcarrier multiplexing,” *IEEE Journal on Selected Areas in Communications*, vol. 39, pp. 2864-2877, 2021.

[6] M. Klinkowski *et al*., “Elastic spectrum allocation for time-varying traffic in flexgrid optical networks,” *IEEE Journal on Selected Areas in Communications (JSAC)*, vol. 31, pp. 26-38, 2013.